ISSN 0031-918X, The Physics of Metals and Metallography, 2013, Vol. 114, No. 2, pp. 108–115. © Pleiades Publishing, Ltd., 2013.
Original Russian Text © V.V. Zverev, B.N. Filippov, 2013, published in Fizika Metallov i Metallovedenie, 2013, Vol. 114, No. 2, pp. 120–128.

THEORY OF METALS

Simulation of Three-Dimensional Micromagnetic Structures in Magnetically Uniaxial Films with In-Plane Anisotropy: Static Structures

V. V. Zverev[a] and B. N. Filippov[a, b]

[a] *Ural Federal University, ul. Mira 19, Ekaterinburg, 620002 Russia*
[b] *Institute of Metal Physics, Ural Branch, Russian Academy of Sciences, ul. S. Kovalevskoi 18, Ekaterinburg, 620990 Russia*
e-mail: vvzverev49@gmail.com

Received July 02, 2012

Abstract—The possible types of transition structures that can arise between the regions of vortex asymmetric domain walls that exist in magnetically uniaxial permalloy films with in-plane anisotropy have been studied by the method of three-dimensional computer simulation of the magnetization behavior. It has been established that, along with the previously found structures of vertical Bloch lines (VBLs), other types of structures can exist, namely, singular (Bloch) points and clusters that consist of VBLs and Bloch points. Spatial configurations and topological characteristics of transition structures have been calculated numerically.

Keywords: magnetic films, micromagnetism, domain walls, Bloch lines
DOI: 10.1134/S0031918X13020142

INTRODUCTION

Locally inhomogeneous magnetization structures and their dynamic properties play a key role in the formation of practically important properties (magnetic losses, hysteresis, etc.) in materials with magnetic ordering. It is known that the characteristic dimensions of these structures, which are large-scale with respect to interatomic spacings of the crystal lattice, are at the same time small from the macroscopic point of view. This makes it possible to employ a micromagnetic approach, in which the energy of a magnet is determined phenomenologically and the magnetization is assumed to be a classical continual vector field. The basis of this approach was laid in the fundamental work by Landau and Lifshitz [1], where they formulated the principle of minimum free energy, and indicated a way to obtain equations of motion, and obtained results for a one-dimensional domain wall. Although later, with the accumulation of experimental data [2] obtained for samples of finite dimensions (in particular, for films), it became clear that the one-dimensional structures are nontypical and only arise if special conditions [3] are fulfilled, the continual theory of magnetization proved to be very useful and fruitful. A generalized description of this theory for crystals of finite dimensions was presented by Brown [4], who in particular suggested the designation "micromagnetism." In [4], an important role of the magnetostatic interaction was revealed, which proved to be responsible, not only for the existence of the domain structure (as was assumed earlier), but also (along with exchange and magnetoanisotropic interaction) for the concrete type of magnetization distribution in domain walls and other micromagnetic structures (MSs).

The micromagnetic approach was used in calculations of memory devices based on the magnetic recording of information [5]. At present, a significant surge of interest has been observed in micromagnetics investigations of magnetic structures and their dynamic behavior in nanosized samples (disks [6], stripes [7], wires [8], and tubes [9]), which is related to the development of spintronics devices [10] and new-type memory devices [11].

For new technologies for storing and processing of information, the searching for stable MSs, the destruction of which requires that certain energy barriers be overcome, is of practical interest. In particular, MSs refer structures in which the magnetization distribution cannot be made uniform via continuous deformations (topological MSs).

The equations of the micromagnetic theory are substantially nonlinear and can only be solved analytically in a few particular cases. For this reason, as well as due to modern progress in computer technologies, the methods of numerical simulation make up the forefront in this field of physics. The possibility of fulfilling the three-dimensional simulation of the magnetization dynamics [12], which recently arose, makes it possible to consider the formation of magnetic properties of existing substances from more general posi-

tions. In our opinion, at present, we are still far from achieving a complete understanding of the problems of statics and dynamics of domain walls and vertical Bloch lines (VBLs) in magnetic films. In earlier works, the concept of a one-dimensional character of domain walls and two-dimensional character of Bloch lines was used [5]. A two-dimensional numerical simulation of the structure of domain walls in permalloy films 50–200 nm thick has shown that the magnetization distributions in these walls are indeed substantially two-dimensional and appear as asymmetrical vortices in the transverse section [13]. The existence of these walls has been confirmed in a series of experimental investigations (see, e.g., [14]). Later, it has been found that, in dynamic processes, the dynamic structure of a domain wall can undergo substantial reconstructions [15, 16]. Thus, in the case under consideration, the one-dimensional model of the wall cannot be adequate. Based on an analysis of experimental data given in [17, 18], Argyle et al. [17] concluded that three types of MSs can exist that separate regions of domain walls from one another with different asymmetric structures, namely, with different dispositions of vortices (to the left or to the right from the central line of the wall and with the opposite direction of the magnetization rotation in them). This conclusion also indirectly confirmed the existence of walls with a two-dimensional distribution of magnetization. The three-dimensional numerical simulation performed for the first time in [19–22] confirmed the two-dimensional and asymmetric character of the walls and also showed that the transition micromagnetic structures (TMSs) that separate the regions of asymmetric walls are substantially three-dimensional local formations. In these works, the main types of static configurations of TMSs in films of iron [19, 20] and permalloy [21, 22] have been found, including various types of vertical Bloch lines (VBLs).

In this work, by simulating the magnetization distribution in permalloy films 80–140 nm, we have found new types of TMSs, including singular points (SPs) with the values of the homotopic number $\chi = \pm 1$ (which are also called Bloch points [5]); these can be individual SPs, or combined MSs (clusters) containing several SPs and VBLs. Note that the assumption on the presence of SPs in TMSs of the type under consideration was suggested in [18], but in [19–22], no solutions with SPs were found.

FORMULATION OF THE PROBLEM

Consider a magnetically uniaxial film with an in-plane anisotropy and a small quality factor $Q \ll 1$. Let the y and z axes be parallel to the film surface, let the x axis be perpendicular to this surface, and let the z axis lie along the easy axis (EA). We will search the equilibrium distribution of the magnetization by minimizing the total energy of the wall that has the following form:

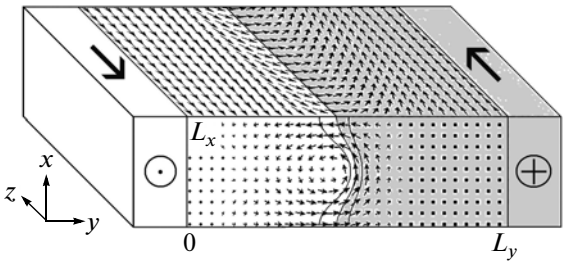

Fig. 1. Magnetization distribution in a vortex asymmetrical domain wall.

$$E = \iiint_V (w_e + w_a + w_m)\, d\mathbf{r}, \tag{1}$$

where

$$w_e = A\left\{\left(\frac{\partial \mathbf{m}}{\partial x}\right)^2 + \left(\frac{\partial \mathbf{m}}{\partial y}\right)^2 + \left(\frac{\partial \mathbf{m}}{\partial z}\right)^2\right\},$$
$$w_a = -K(\mathbf{km})^2, \tag{2}$$
$$w_m = -\frac{1}{2} M_s \mathbf{m}\mathbf{H}^{(m)}$$

are the densities of the exchange energy, anisotropy energy, and magnetostatic energy expressed through the normalized magnetization $\mathbf{m} = \mathbf{M}/M_s$ ($|\mathbf{m}| = 1$). The magnetostatic field $\mathbf{H}^{(m)}$ is determined as usual, i.e., as a solution to the equations of magnetostatics, with corresponding boundary conditions. We consider a sample in the form of a parallelepiped with edges L_x (film thickness), L_y, and L_z. On the film surfaces, $x = 0$ and $x = L_x$, the magnetization is not fixed, and the usual boundary conditions are fulfilled [4]. On the other faces of the parallelepiped, magnetization obeys the following relationships:

$$\mathbf{m}\big|_{y=0} = -\mathbf{k}, \quad \mathbf{m}\big|_{y=L_y} = \mathbf{k}; \tag{3}$$

$$\mathbf{m}\big|_{z=0} = \mathbf{m}\big|_{z=L_z}. \tag{4}$$

The imposition of periodic boundary conditions (analogous to the Born–Kármán conditions) along the z axis makes it possible to avoid the consideration of effects related to the magnetization cutoff at surfaces perpendicular to the domain wall. When calculating the magnetostatic field, it is assumed that, along the z axis, there is an infinite chain of regions with a similar distribution of magnetization (upon the summation of contributions from remote regions, the magnetization is approximated by a one-dimensional continual distribution; this makes it possible to avoid the cutoff of the summation process [23]).

The structure of an asymmetric Bloch (C-like) domain wall that separates the domains in which the magnetization has the orientation $\mathbf{m} = \pm\mathbf{k}$ is shown in Fig. 1. The magnetization distribution on the film surface coincides with that in a Néel wall, but in the sec-

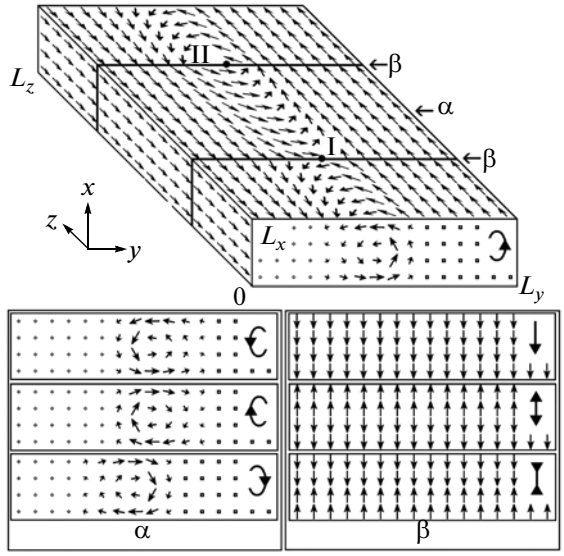

Fig. 2. Constructing initial distributions (schematic). Pictograms in the form of open ovals with arrows and vertical arrows are stylized images of various types of magnetization distribution in sections perpendicular to the z axis and serve to index them.

tion by the plane perpendicular to the z axis, it proves to be vortex-like. In the figure, the regions where $m_z(\mathbf{r}) > 0$ are painted in gray. Inside the domain wall, the boundary of this region is the central surface of the wall, $m_z(\mathbf{r}) = 0$; the intersection of this surface with the plane $x0y$ has the form of a curve that separates painted and unpainted regions at the butt surface of the sample (the two other curves are determined by the equations $m_z(\mathbf{r}) = \pm 0.3$). We see that the axis of the vortex formation lies to the left of the wall center (left-hand wall). This spatial distribution of magnetization makes it possible to almost completely close the magnetic flux inside the sample and decrease the magnetostatic energy. In this case, no regions with strong inhomogeneities (magnetization jumps) arise and the exchange energy remains fairly small.

By making a 180° rotation about the x axis, from the domain wall shown in Fig. 1, we obtain a right-hand wall with an opposite direction of the vortex rotation. Another transformation (inversion $\mathbf{m} \to -\mathbf{m}$ and the subsequent mirror reflection relative to the plane $x0y$) leads to a change in the direction of the vortex rotation, which remains the left-hand wall. By combining these transformations, we can convert a left-hand wall into a right-hand wall without changing the type of the vortex rotation. Thus, there are four configurations of a wall connected by symmetry transformations and have the same energies (fourfold degeneracy with respect to the magnetization configurations). Due to the effect of some external factor or the prehistory of the system, the situation can occur when the neighboring regions of asymmetric walls can differ from one another. By arbitrarily choosing the

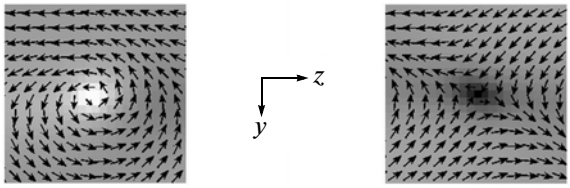

Fig. 3. Surface structures of vortex (left) and antivortex (right) types.

magnetization configuration in some region of the wall, we should search for TMSs, which permit us to proceed from this configuration to each of the other configurations that can arise in adjacent regions of the wall. It is understandable that there are at least three types of TMSs [19–22], among them various types of VBLs.

In this work, we employed the following approach: using numerical simulation, we will search for magnetization distributions with predetermined characteristics. These distributions can be found using the procedure of energy minimization for specially chosen initial distributions. The process of searching for solutions is shown schematically in Fig. 2. At the first stage, the piecewise constant distribution of magnetization is chosen as initial, which roughly imitates the distribution of $\mathbf{m}$ in an asymmetrical domain wall. Then, a two-dimensional distribution that is translation-invariant relative to the z axis is calculated by minimizing the energy; it corresponds to a left-hand domain wall. At the second stage, in the α region, which lies between the β planes, the magnetization distribution is transformed in one of the three above-described ways. The transverse section of each of the thus-obtained distributions is given in the bottom part of Fig. 2 in the left-hand panel.

It can be noted that, in the middle part of the wall, on the surface of the film, after carrying out the above-described transformations, the directions of the magnetization vectors on the opposite sides of any plane β either coincide or are opposite. It has been shown in [19–22] that, in the last case, the structures of the vortex and antivortex types are formed on the boundary surfaces of the film (Fig. 3); in particular, on the surface $x = L_x$, they are located near points I and II (Fig. 2). In the vicinity of the centers of the vortices (antivortices), there are regions with a maximum $|m_x| \sim 1$. We will call them magnetostatic poles (the term "pole" will only be used in this work with this narrow meaning). In Fig. 3, the degree of darkening is proportional to the magnitude of m_x; in the center of the vortex, we have $m_x = 1$; in the center of the antivortex, $m_x = -1$, so that the magnetostatic pole has the form of a light or dark spot (note that there can also exist a vortex with $m_x = -1$ and an antivortex with $m_x = 1$). It will be shown below that the configurations of magnetization distributions in TMSs that have poles with dif-

ferent signs of m_x are different. In this work, we restrict ourselves to studying TMSs that have no more than one magnetostatic pole on each boundary surface of the film. In order to calculate the magnetization configurations by controlling the magnitudes of m_x in the poles, when forming the initial magnetization distributions, it is sufficient to introduce two types of thin layers along the planes β, (a) with $m_x = 1$ or $m_x = -1$ over the entire layer; or (b) with $m_x = \pm 1$ at $0 < x < \frac{1}{2}L_x$ and $m_x = \mp 1$ at $\frac{1}{2}L_x < x < L_x$ (three variants of distributions in β layers are given in Fig. 2 in the right-hand panel). After the completion of the formation of initial distributions, for each of them, the energy minimization is performed for the second time. As a result, in the vicinities of planes β, we obtain the sought MSs that separate regions of domain walls.

If we assume that the index j of the plane contour Γ on the film surface corresponds to the number of turns of the tangential component of the vector **m** upon the bypass of the contour ($j > 0$ if the magnetization rotates in the direction of the bypass; $j < 0$ in the opposite case), if there is a vortex inside the contour, we have $j = 1$; in the case of an antivortex, $j = -1$; if there is a vortex + antivortex pair or no structures of this type exist inside the contour, $j = 0$. This means that a vortex and an antivortex are topological MSs; these structures cannot be destroyed via continuous deformations, but the annihilation of the vortex + antivortex pair is possible.

The calculations were performed using values of the substance parameters characteristic of permalloy films of zero-magnetostriction composition: $A = 10^{-11}$ J/m, $K = 10^2$ J/m^3, $M_s = 800$ G. The dimensions of the samples were as follows: L_x =80–140 nm, L_y = 400 nm, L_z = 750 nm. For the numerical minimization of the energy, the method of conjugate gradients was employed (based on the Fletcher–Reeves algorithm) realized in an OOMMF program package [12] with a discretization on a rectangular grid with a step of 5 nm in each coordinate (the grid step does not exceed the dimension of the absolute single-domainness $l = \sqrt{A/2\pi}/M_s$). The distance between the planes β was chosen to be equal to $\frac{1}{2}L_z$.

RESULTS AND DISCUSSION

The results of calculations are given schematically in the table in the form of pictograms introduced in Fig. 2. The asterisks correspond to singular points (SPs); symbols *X* and *Y* denote various types of VBLs. The sequence of pictograms read from left to the right corresponds to the order of the elements of an MS and of regions of domain walls upon the scanning of the sample along the *z* axis in the positive direction. The A,

Configurations of initial distributions (IDs) and corresponding configurations of TMSs obtained by energy minimization

Type of MSs	ID	Resulting TMSs	
A		I	
		II	
B		I	
		II	
C		I	
		II	
B_1		I	
		II	
C_1		I	
		II	
C_2		I	
		II	
C_3		I	
		II	
C_4		I	
		II	

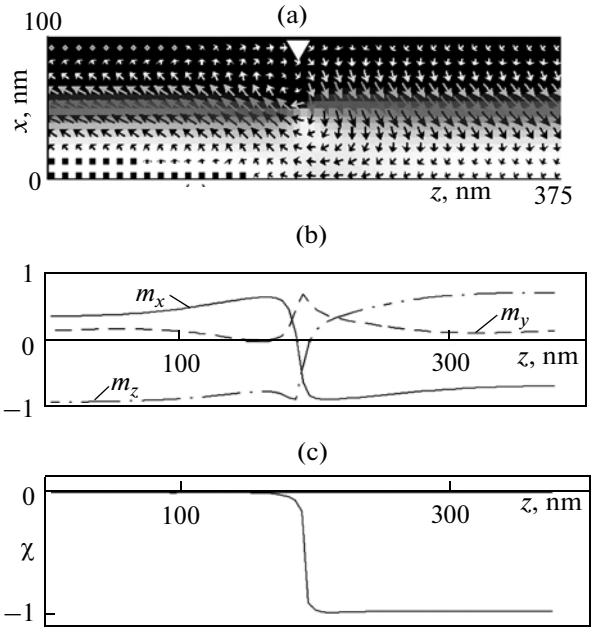

Fig. 4. Transition region between domain walls that contains a singular (Bloch) point.

B, and C configurations differ from one another in the type of the domain wall in that part of the sample that lies between the β planes (Fig. 2). The TMS localized near planes (β, I) and (β, II) correspond to I and II in the table. Consider various particular types of MSs in more detail.

In case A, the TMS separates left-hand and right-hand walls that represent vortex tubes in which the directions of the vortex twisting are the same and the magnetization directions in the near-axis regions are opposite. No VBLs and poles arise at the film boundaries in the case of such a magnetization configuration, but in the vicinities of β planes, two SPs are formed at the sites of the connection of the axes of vortex tubes. On the grid, an SP appears as a local region in which the angles between the magnetization vectors at neighboring sites are not small. Figure 4a displays a section of the part of the sample located between the planes $z = 0$ and $z = 375$ nm by the plane $y = 200$ nm; the location of the SP is indicated by a white triangle (here and below the intensity of gray is proportional to **mv**, where **v** is the unit vector of the coordinate axis perpendicular to the plane of the figure; the lighter tint corresponds to greater values of **mv**. The one-dimensional distribution of magnetization on a straight line $x = 50$ nm, $y = 200$ nm, which passes through the SP has a finite discontinuity (Fig. 4b). In order to determine the exact position and type of the SP, one should find its homotopic number as a function of the coordinate z. Let us use the representation of this quantity in the form of a surface integral [5]

$$\chi(\varsigma) = \frac{1}{4\pi}\oint_{S(\varsigma)} \mathbf{g}(\mathbf{r})d\mathbf{s}, \quad \mathbf{g}(\mathbf{r}) = \frac{\nabla m_\alpha \times \nabla m_\beta}{m_\gamma}, \qquad (5)$$

by expressing the density of the gyrotropic vector **g** through the Cartesian coordinates of the magnetization $(\alpha, \beta, \gamma) = (x, y, z)$, or (y, z, x), or (z, x, y). We will assume that $S(\varsigma)$ is the boundary surface of the parallelepiped $V(\varsigma) = ((x, y, z)$, where $0 < x < L_x$, $0 < y < L_y$, $0 < z < \varsigma)$. The calculated $\chi(z)$ dependence is shown in Fig. 4c. Upon an increase in ς, we see that, at the moment when ς becomes equal to the coordinate z of the SP, a jumplike change occurs in $\chi = 0 \to -1$ caused by the fact that the SP entered into the region $V(\varsigma)$. The smooth character of the change of the function $\chi(z)$ found numerically (Fig. 4c) can be explained by the fact that the singularity in the grid is smeared.

In case B, the transition regions between the domain walls represent VBLs of X type (of type T1 in the designations used in [22]) located near the β planes. On the opposite boundaries of the film, each VBL has a vortex and an antivortex in the centers of which the directions of the magnetization vectors are the same and perpendicular to the film boundaries. Considering a series of sections $z = \text{const}$ at various values of z, we see that, near the VBL, the central surface of the wall $m_z(\mathbf{r}) = 0$ becomes flattened and the near-axis region of the vortex of the domain wall is shifted toward the nearest domain (Fig. 5a) and merges with it, which leads to the destruction of the vortex tube. The process of the vortex destruction on one side of the central surface of the domain wall is accompanied by the generation of a vortex on the other side; the near-axis region with the opposite value of m_z is separated from the second domain and proves to be surrounded by a new vortex tube (Fig. 5c). In the section $z = 180$ nm passing through the center of the VBL (Fig. 5b), there arises a symmetric two-vortex structure. The magnetization distribution in the section $y = 200$ nm has a characteristic crosslike form (Fig. 5e). It can be seen from Fig. 5d that, on opposite sides of the VBL, the center of the wall lies closer to different domains.

In case C, in the vicinities of the planes, Y-type VBLs arise (in the designations used in [22], type T2) with a more complex structure of the magnetization distribution. Now, in the centers of the vortex and antivortex formed at different film boundaries, the magnetization vectors are perpendicular to the film boundaries and are directed in the opposite directions. It can be seen from Figs. 6a and 6b that the destruction of the left-hand wall twisted counterclockwise occurs when the near-axis region of this tube goes onto the upper boundary of the film. With movement in the positive direction of the z axis, we can observe on

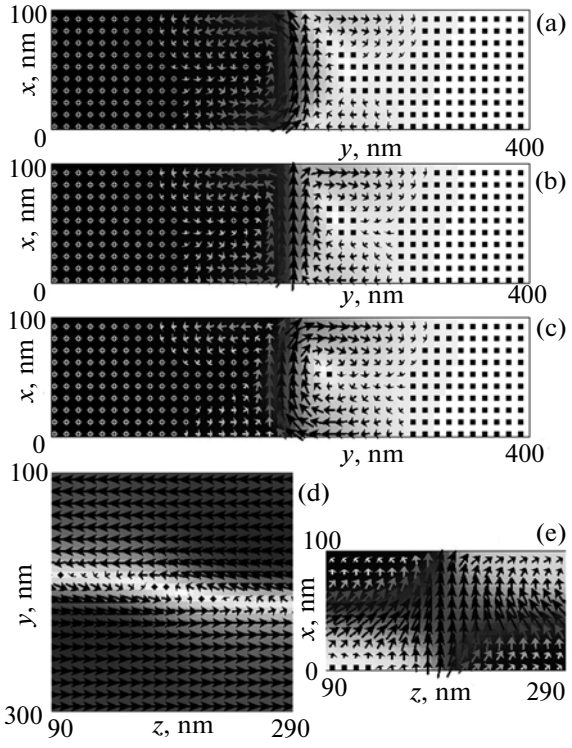

Fig. 5. Configurations of magnetization for VBLs of *X* type in sections of the sample by planes (a) $z = 160$, (b) 180, (c) 200, (d) 50 nm, and (e) $y = 200$ nm.

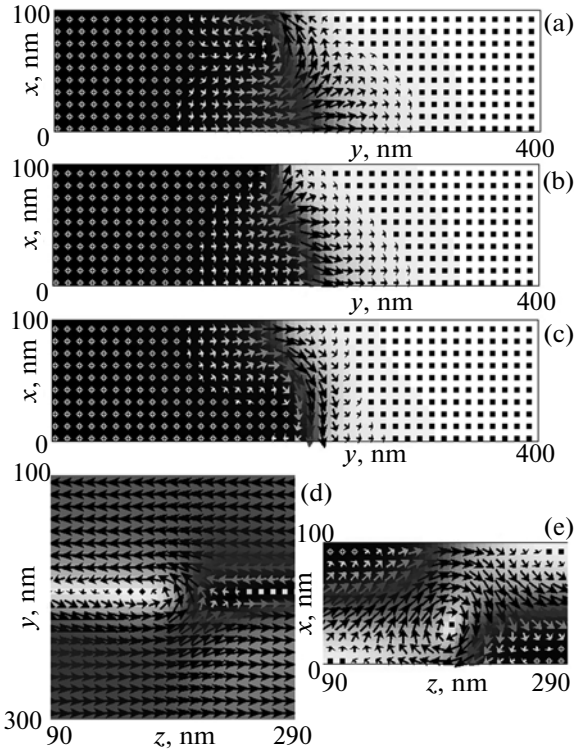

Fig. 6. Configurations of magnetization for VBLs of *Y* type in sections of the sample by planes (a) $z = 170$, (b) 182, (c) 195 nm, (d) $x = 50$ nm, and (e) $y = 200$ nm.

the lower boundary surface the formation of a near-axes region of the vortex tube of a left-hand wall but with the vortex twisted clockwise (Fig. 6c). In the section by the plane $y = 200$ nm, the VBL of the *Y* type has a transverse vortex structure (Fig. 6e), which makes it possible to obtain poles with opposite magnetization vectors on the film boundaries in the absence of a Bloch point between the poles. Two subtypes of this type of VBL are possible, which differ in the direction of the magnetization vector in the center of the vortex shown in Fig. 6e; in the table, they are designated as *Y* and $\bar{Y}$.

The B_1(II), C_1(I), C_2(I,II), and C_4(I,II) structures are clusters that consist of VBLs of *X* type and one or two SPs. Figures 7a and 7c show the sections of the magnetization distribution for the TMSs C_2(I) and B_1(II) by the plane $y = 200$ nm; the white triangles indicate the positions of the SPs. A corresponding graph of the function $\chi(z)$ is given in each section. We see that, for the SP that contains in C_2(I), $\chi = -1$ (Fig. 7b) and, for each of the two SPs that contain in B_1(II), $\chi = 1$ (Fig. 7d). The nonmonotonicity of the $\chi(z)$ function at the place where the VBL is located appears to be explained by the errors inherent in the finite-difference approximation.

The stability of clusters containing SPs is checked as follows: the fields **m** that describe them were summed with the random field $\mathbf{m}_r$ ($|\mathbf{m}_r| \sim 0.5$). The thus-obtained fields were normalized, after which the energy was repeatedly minimized. As a result, magnetization distributions were obtained that negligibly differed from the initial distributions.

In the geometry under consideration, at a film thickness $L_x < 150$ nm, the interaction of TMSs located at distances on the order of $L_z/2 = 375$ nm from one another can be considered to be weak. It follows from Fig. 8a that the energy of the domain wall without a TMS is the smallest; i.e., a wall with any type of TMS is in a metastable state. Note that this result disagrees with the conclusions that usually are obtained when considering magnetically uniaxial films with an easy axis that lies in the film plane in the one-dimensional model of the magnetization distribution. It can be concluded that this discrepancy indicates the inadequacy of the one-dimensional model. From the viewpoint of a one-dimensional approach, VBLs should be stable, since they decrease the poles at the boundary surfaces of the film in stripes formed by the intersection of a domain wall with these surfaces. In more realistic models, which allow for the two-dimensional and three-dimensional character of the magnetization distributions, vortex-like formations with Néel regions can appear on the film surfaces. In this case, the magnetic flux is almost completely closed inside the film, which leads to the disappearance of the cause of the gain in energy due to the pres-

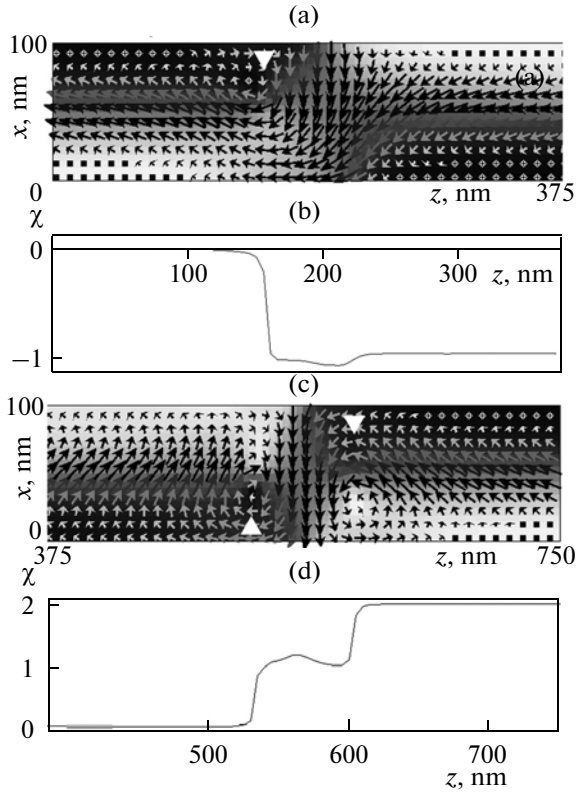

Fig. 7. Clusters that consist of VBLs of *X* type and one or two singular points: (a, c) sections of the magnetization distributions by the plane $y = 200$ nm; (b, d) corresponding graphs of the function $\chi(z)$.

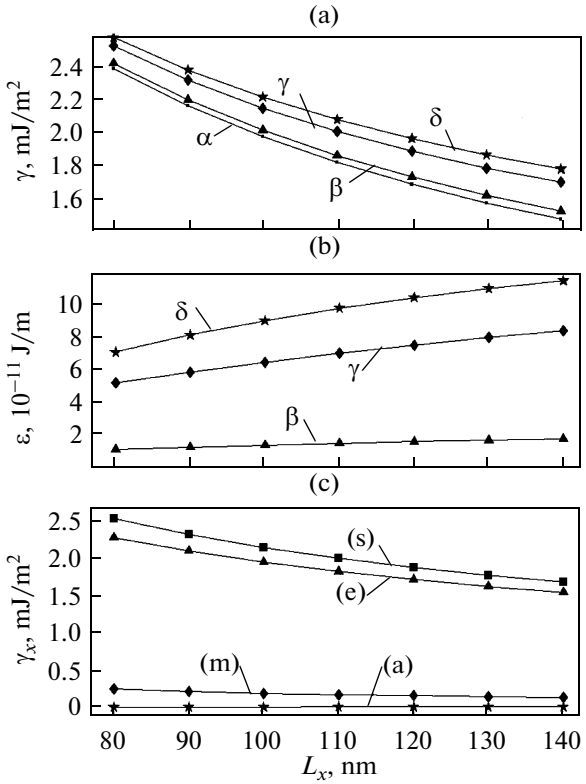

Fig. 8. Effect of film thickness on (a) surface densities of energy for a wall of the (α) type without a TMS or (β, γ, δ) with two TMSs; (b) on the energies of TMSs referred to the film thickness; and (c) on the surface densities of partial energies for a film with two VBLs of *X* type. Data correspond to walls with SPs (β), VBLs of *X* type (γ), and VBLs of *Y* type (δ). Family of curves (c) consists of graphs of the (s) total, (e) exchange, (m) magnetostatic, and (a) anisotropy energy.

ence of VBLs. Nevertheless, as follows from experimental works, various types of TMSs do really exist (see, e.g., [17, 18]). It is natural to consider that their appearance is related to the prehistory of the formation of the domain structure on the whole. In addition, VBLs can be produced artificially, e.g., by applying inhomogeneous pulsed magnetic fields to the film.

It can be seen from Fig. 8b that the energies of VBLs and SPs per unit of the film thickness increase with increasing film thickness. This indicates that, because of the three-dimensional nature of these formations, their change upon transferring to thicker films is not reduced to merely their elongation.

The curves of the densities of partial energies shown in Fig. 8c for a particular case of an *X*-VBL are typical; approximately the same proportions between partial energies are also observed for other TMSs. It can be seen that the main contribution comes from the exchange energy. Because of the fairly good closure of the magnetic flux, the contribution from the magnetostatic energy proves to be significantly smaller. The contribution from the anisotropy energy also is small because of the smallness of the quality factor of the films under consideration.

It follows from the data obtained that, in spite of the metastable character of TMSs, they can be considered as promising elements for high-density magnetic recording. The variety of the TMS types and the possibility of controlling transitions between them permit us to hope for their successful application in logic devices.

CONCLUSIONS

In this work, we used numerical simulation with an exact allowance for all main interactions in magnetically uniaxial films with in-plane anisotropy (including dipole–dipole one) to find three-dimensional micromagnetic structures of the magnetization distribution **m** that separate regions of asymmetric vortex-like walls with a different disposition of vortices and/or different magnetization rotations in these vortices.

It has been shown that the three possible types of transitions between the regions of walls of different types correspond to three basis structures, including singular (Bloch) points (SPs) and vertical Bloch lines (VBLs) of types *X* and type *Y*. The data of [21, 22],

which indicate that, at the sites of the localization of VBLs at the boundary surfaces of the film, vortices and antivortices can exist in the centers of which the magnetization vectors are codirectional in the *X* structures and opposite in the *Y* structures, have been confirmed. A numerical analysis of the changes in the structure of the magnetization in planar sections that are observed when going from one region of the asymmetrical vortex-like wall to another has been performed, i.e., the micromagnetic structure of three-dimensional VBLs and SPs has been described. The possible structures of clusters consisting of VBLs and SPs have also been described.

Based on the numerical data obtained, the homotopical numbers (topological charges) of the isolated SPs and SPs entering into clusters have been found.

It has been shown that asymmetrical domain walls containing VBLs, SPs, and clusters are metastable. However, being topological structures, they are fairly stable and additional energy expenditure is required to destroy them. At the same time, the only stable domain-wall formation is an asymmetrical vortex Bloch wall.

It has been revealed that, irrespective of the type of the TMS, the total energy of the asymmetrical Bloch walls decreases with increasing film thickness, which is mainly related to the decrease in the exchange energy due to the decrease in the degree of the inhomogeneity of magnetization in thicker films.

For the first time, we found the partial contributions of various energies to the total energy of asymmetrical Bloch walls containing TMSs. It has been shown that, just as in the case of walls without TMSs, the main contribution to the total energy comes from the inhomogeneous exchange interaction.

ACKNOWLEDGMENTS

This work was supported in part by the Russian Foundation for Basic Research (project no. 11-02-00931).

REFERENCES

1. L. Landau and E. Lifshitz, "On the Theory of the Dispersion of Magnetic Permeability in Ferromagnetic Bodies," Phys. Z. Sow. **8**, 153–159 (1935).
2. A. Hubert and R. Schäfer, *Magnetic Domains: The Analysis of Magnetic Microstructures* (Springer, Berlin, 1998).
3. L. Néel, "Some Properties of Boundaries between Ferromagnetic Domains," Can. J. Phys., **25** (1), 1–20 (1944).
4. W. F. Brown, *Micromagnetics* (Wiley–Interscience, New York, 1963; Nauka, Moscow, 1979).
5. A. Malozemoff and J. C. Slonczewski, *Magnetic Domain Walls in Bubble Materials* (Academic, New York, 1979; Mir, Moscow, 1982).
6. R. P. Cowburn, D. K. Koltsov, A. O. Adeyeye, M. E. Welland, and D. M. Tricker, "Single-Domain Circular Nanomagnets," Phys. Rev. Lett. **83**, 1042–1045 (1999).
7. J.-Y. Lee, K.-S. Lee, S. Choi, K. Y. Guslienko, and S.-K. Kim, "Dynamic Transformations of the Internal Structure of a Moving Domain Wall in Magnetic Nanostripes," Phys. Rev. B:Condens. Matter Mater. Phys. **76**, 184408 (2007).
8. R. Varga, K. Richter, A. Zhukov, and V. Larin, "Domain Wall Propagation in Thin Magnetic Wires, "IEEE Trans Magn. **44**, 3925–39–30 (2008).
9. M. Yan, C. Andreas, A. Kakay, F. Garcia-Sanchez, and R. Hertel, "Fast Domain Wall Dynamics in Magnetic Nanotubes: Supression of Walker Breakdown and Cherenkov-like Spin Wave Emission," Appl. Phys. Lett. **99**, 122505 (2011).
10. H. Zabel, "Progress in Spintronics," Superlattices Microstruct. **46**, 541–553 (2009).
11. S. S. P. Parkin, M. Hayashi, and L. Thomas, "Magnetic Domain-Wall Racetrack Memory," Science **320**, 190–194 (2008).
12. M. J. Donahue and D. G. Porter, *OOMMF User's Guide, Version 1.0 NISTIR 6376* (National Institute of Standards and Technology, Gaithersburg, Md, 1999).
13. A. E. LaBonte, "Two-Dimensional Bloch-Type Domain Walls in Ferromagnetic Films," J. Appl. Phys. **40**, 2450–2458 (1969).
14. J. N. Chapman, G. R. Morrison, J. P. Jakubovics, and R. A. Taylor, "Determination of Domain Wall Structures in Thin Foils of a Soft Magnetic Alloy," J. Magn. Magn. Mater. **49** 277–285 (1985).
15. S. W. Yuan and H. N. Bertram, "Domain-Wall Dynamic Transitions in Thin Films, Phys. Rev. B: Condens. Matter **44**, 12395–12405 (1991).
16. B. N. Filippov, "Static Properties and Nonlinear Dynamics of Domain Walls with an Internal Vortex Structure in Magnetic Films, Fiz. Nizk. Temp. **28**, 991-1032 (2002).
17. B. E. Argyle, B. Petek, M. E, Re, F. Suits, and D. A. Herman, "Bloch Line Influence on Wall Motion Response in Thin-Film Heads," J. Appl. Phys. **63**, 4033–4035 (1988).
18. C. G. Harrison and K. D. Leaver, "The Analysis of Two-Dimensional Domain Wall Structures by Lorentz Microscopy," Phys. Status Solidi A **15**, 415–429 (1973).
19. S. Huo, J. E. L. Bishop, J. W. Tucker, W. M. Rainforth, and H. A. Davies, "3-D Simulation of Bloch Lines in 180° Domain Walls in Thin Iron Films," J. Magn. Magn. Mater. **177–181**, 229–230 (1998).
20. S. Huo, J. E. L. Bishop, J. W. Tucker, W. M. Rainforth, and H. A. Davies, "3-D Micromagnetic Simulation of a Bloch Line between C-Sections of a 180° Domain Wall in a {100} Iron Film," J. Magn. Magn. Mater. **218**, 103–113 (2000).
21. M. Redjdal, A. Kakay, T. Trunk, M. F. Ruane, and F. B. Humphrey, "Simulation of Three-Dimensional Nonperiodic Structures of a π-Vertical Bloch Line (pi-VBL) and 2π-VBL (2pi-VBL) in Permalloy Films," J. Appl. Phys. **89**, 7609–7611(2001).
22. M. Redjbal, A. Kakay, M. F. Ruane, and F. B. Humphrey, Magnetic Domain Wall Transitions Based on Chirality Change and Vortex Position in Thin Permalloy Films, J. Appl. Phys., **91**, 8278–8280 (2002).
23. K. M. Lebecki, M. J. Donahue, and M. W. Gutowski, "Periodic Boundary Conditions for Demagnetization Interactions in Micromagnetic Simulations," J. Phys. D: Appl. Phys., **41**, 175005 (2008).